IOP Conf. Series: Materials Science and Engineering **418** (2018) 012054 doi:10.1088/1757-899X/418/1/012054

Determination and Application of Forming Limit Diagram of Aluminium Alloy 5083 Sheet

Gang Fang [a,*], Jia-Qing Zhao [b], Qian Wang [a]

[a] State Key Lab of Tribology, Department of Mechanical Engineering, Tsinghua University, Beijing, 100084, China
[b] Institute of Nuclear and New Energy Technology, Tsinghua University, Beijing 100084, China.

E-mail: fangg@tsinghua.edu.cn

Abstract. The present research was aimed to evaluate the formability of aluminium alloy 5083-O sheet. Two-dimensional DIC method was used to measure the strain field of uniaxial tensile specimens. The flow stress equation was obtained on the base of these measured strain and stress data. The influence of virtual gauge on strain measurement was analysed. The hemispherical punch tests were conducted, where three-dimensional DIC was used to measure the strains on the forming regions of aluminium sheets. The FLD of aluminium alloy 5083-O was established using these measured strain data. The data derived from the tests were applied in FE simulations of the inner panel of a car body. Comparison between the results of the experiments and the simulations showed that the necking and fracture of the aluminium alloy component during stamping could be accurately predicted.

1. Introduction

To reduce the fuel consumption, the application of light-weight structural materials such as aluminium alloys has become one of the hot spots in automobile industry [1]. Thanks to their excellent properties of high specific-strength, good corrosion resistance and weldability, aluminium-magnesium (Al-Mg) alloy sheets are extensively used in the automotive industry, as the substitute of steel sheets. Traditionally, the aluminium parts of a car, such as engines, wheels, exhaust decor, were produced by casting. Nowadays, more and more wrought aluminium products in sheets are applied in the car body, such as exterior panels, door and heat insulators. Compared with the mild steel sheet, the aluminium alloy sheet has lower formability, higher springback and surface sensitivity when it comes into contact with forming die or tool [2]. Therefore, the warm or hot forming of aluminium alloys was employed [3, 4]. Some new problems, which arise from the heating of tool and sheet and the microstructure evolution of the formed sheet, are encountered in the warm or hot forming of aluminium alloy sheet. However, given the low cost, high efficiency and good performance of the product, the forming at room temperature is still favoured.

Some exterior and inner panels of an automotive body are formed primarily by stretching. Forming limit diagram (FLD) characterizes the formability of a sheet material undergoing strains to necking failure. Traditional methods of strain measurement by marking or etching grids on the surface of a metal sheet lead to low resolution and measurement accuracy [2]. Recently, the digital image correlation (DIC) technology has been applied in the measurement of strain field and proved to be superior to the

traditional methods [3,4]. Combined with the CCD (charge-coupled device) image acquiring technology and computer image analysis, DIC becomes a new full-field strain measurement method [5,6].

The present research aims at evaluating the formability of aluminium alloy 5083-O sheet. It is an aluminium alloy of the non-heat treatable Al-Mg with optimum strength and corrosion resistance and is used in the automotive body. The 2-D DIC measurement system was applied in strain measurement during tensile tests. The ball punch deformation was used to gain complex strain fields, and a 3-D DIC measurement system was applied to record the strain variation in deformation region. The necessary investigation into the formability of sheet material contributes to its forming process designs of auto body components.

2. Experimental procedure

2.1. Tensile tests

All specimens used in this investigation were made of rolled sheets of aluminium alloy AA5083-O. The tensile tests were conducted at room temperature, and tensile speed 0.015mm/s was used on a servo-hydraulic material test machine (Shimazu, Japan). The self-developed 2-D DIC measurement system was applied during the tensile test. Some speckles were painted on the surface of the aluminium alloy sheet, and their displacement were tracked by a CCD and recorded by a computer. The variation of strain field with time was calculated by the program [5]. The tensile forces were measured by the testing machine. According to the Standard GB/T 228.1-201, dog-bone-shaped sheet specimens with a thickness of 1.5 mm were cut and tensioned along 0° (RD), 45° and 90º (TD) to rolling directions of the sheet.

2.2. Ball punch deformation tests

The ball punch deformation tests were prepared and conducted according to the standard ASTM E643-09. Figure 1a shows the schematic of die set-up. The radius of the hemispherical punch was R1 = 9.95 mm. The diameter of the sheet was D1 = 70 mm. The diameter of the die was D = 23 mm and its corner radius was R2 = 0.8 mm. The blank holder was a ring with an inner radius of D3 = 33.1mm. To obtain forming paths between the uniaxial stretching and the equal-biaxial stretching, some waisted samples were prepared (Figure 1b). Between the aluminium alloy sheet and the die and the blank holder, there was no lubricant. Vaseline as a lubricant was painted on the surface of the punch before the punching. During the test, the hemispherical punch travelled upwards and drew the sheet into the die cavity, and the holder force on the blank sheet was maintained a constant. By this self-developed test machine, the punch stopped automatically when the force sensor detected the descending of the load. The deformation images of the specimen with speckles were captured synchronously by two CCDs of the DIC system [5]. The strain field on the outside surface of the bulged specimen was calculated according to the recorded displacements of the speckles.

2.3. Validation of speckle pattern and strain accuracy

The speckle pattern (i.e. the speckle size and density) has an important influence on the measurement accuracy of strain using DIC. Typical speckle pattern used in the present tensile and bulging test is shown in Figure 2a. To verify the strain accuracy with this type of speckle pattern, the simulated test rather than real experiment was performed to exclude the environment influence and different sources of experimental errors. Firstly, one typical image in tensile test was selected as the deformed image, and then a reference image was generated using Lu's method [7] by applying the sigmoid displacement function $u = 20/(1 + e^{-0.06x})$ onto each pixel where u was prescribed displacement on x direction in image coordinate. Both images were added with zero-mean Gaussian random noise with standard deviation of two grey-scales, which was statistically computed based on the CCD cameras. The grey-scale of each pixel was obtained by cubic B-spline interpolation. The sigmoid function is a step function which is suitable for simulating the strain concentration in the necking during sheet metal forming. Finally, the displacement and strain fields of the centre region (Figure 2a) of 69 by 562 pixels were

computed with our DIC routines, and the second-order shape function and subset size of 21 by 21 pixels were adopted. Figure 2a shows the measured ε_x field, where obvious strain concentration appears near the centre of strain field. Figure 2b and 2c show the comparison between the theoretical and measured mean u and mean ε_x field on each vertical line of deformation field, it could been seen that the measured displacements and strain fields are in good agreement with the theoretical values. For mean u field in Figure 2b, the maximum bias is 1/55 pixels. Figure 2d shows the mean bias and the standard deviation (St.d.) of ε_x by DIC. It reveals that the theoretical maximum strain is 0.3, while the average and the maximum standard deviation is only 0.0013 and 0.0031 (Figure 2d point A) respectively, and the average mean bias is -2.2e-5, while the maximum values is only 0.0058 (Figure 2d point B), which is only 1.9% of the peek value. It is accurate enough for depicting strain evolution and generating a FLD.

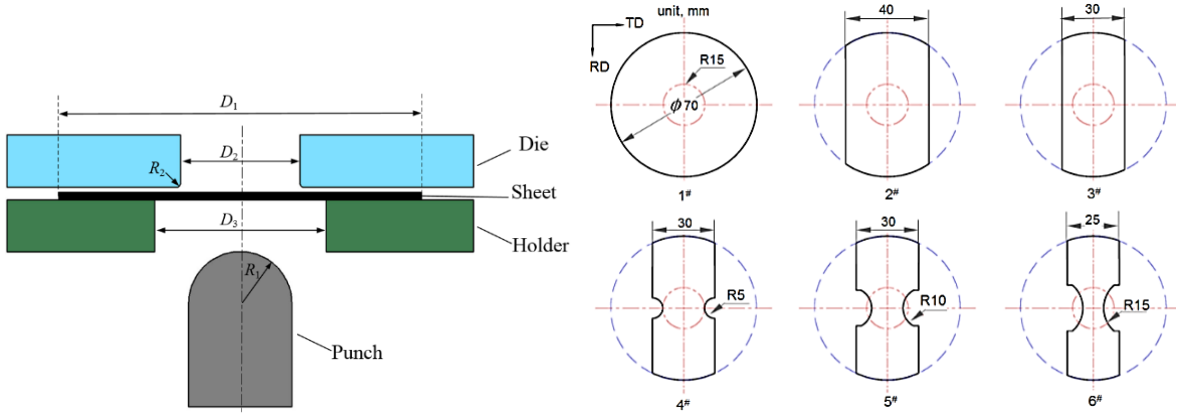

(a) (b)

Figure 1. Shapes and dimensions of (a) dies used for ball punching, (b) samples (thickness: 1.5mm).

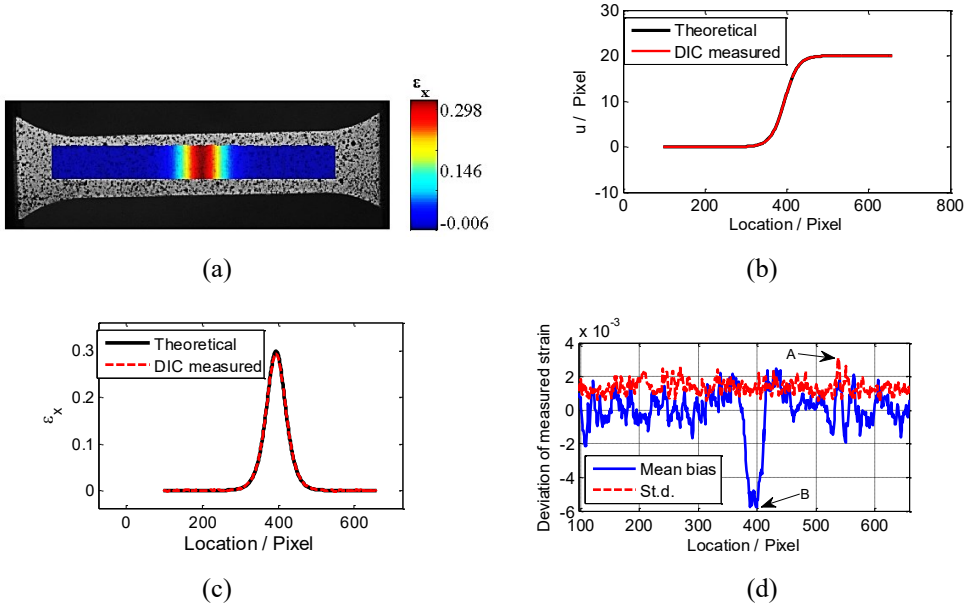

(a) (b)

(c) (d)

Figure 2. Validation of spackle patterm adopted in experiments: (a) Typical speckle pattern and the strain field ε_x measured by DIC, (b) Comparision between the theoretical and measured mean displacement u on each vertical line of the u field, (c) Ccomparision between the theoretical strain and the mean ε_x on each vertical line of the strain field, (d) The mean bias and the standard deviation (St.d.) of the measured ε_x.

3. Results and discussion

3.1. Results of uniaxial tensile tests

The tensile forces were recorded by the test machine. The 2-D DIC system recorded dynamic strain fields and deformation process of the specimens. Figure 3 shows the measured strain distributions, which were captured by the CCD of 2-D DIC system. It can be seen that the strain on the specimen surface increased from both ends to the middle part of the tensile specimen.

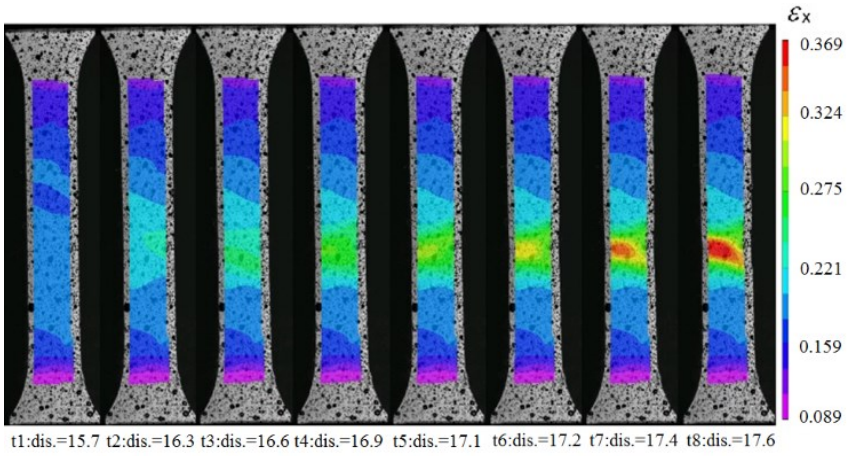

Figure 3. Dynamic strain fields (in tensile direction) of a tensile specimen.

Generally, the strain measurement of a tensile test depends on an extensometer, which records the change of the gauge length. Before a tensile test, the exact position of necking or fracture is hard to estimate. Therefore, the gauge length has to be considered large enough to cover the failure region. In general, the gauge length is 25mm, 50mm, or 100mm according to the geometry of the tensile specimen. The strain is derived from the change of the gauge length, and it is called averaged one. As shown in Figure 3, the strain distributed unevenly within the deformation area. To obtain the constitutive constants of the tested material, an average strain in the necking region is needed. The accuracy of average strain is influenced by the gauge length. The measurement error increases with the increasing gauge length. When the 2-D DIC system is applied in the strain measurement, the necking or fracture region can be distinguished from the recorded full images. The gauge length used to average strain can be concentrated in a region as small as possible. Figure 4a shows the gauge selection for average strain calculation. Figure 4b shows the calculated true strain varying with the time. The incipient strains calculated using different gauge lengths have little deviation. However, with the development of plastic deformation of the tensile specimen, the difference of the average strains resulted from two gauge lengths becomes more significant. It is can be explained that the large gauge length decreases the deformation concentration degree. By the DIC technology, the rational gauge length can be determined from the recorded strain field, which is a distinguished advantage over the traditional extensometer.

Figure 5 shows three true tensile stress-strain curves in three sampling directions (along 0º, incline 45º and transverse 90º to the rolling direction). Each of the curves was averaged from data of three repeat tensile tests. The elastic properties in different tensile directions of the rolled and annealed sheet of aluminium alloy 5083 were almost same. By calculation, the values of r_0, r_{45} and r_{90} (thickness anisotropic index in three sampling directions) were 0.816, 0.560 and 0.683, respectively. In-plane anisotropy of this alloy was also not significant, and the flow stress in rolling direction was a little higher than that in other two directions. It also showed that the elongations in three direction are slightly different.

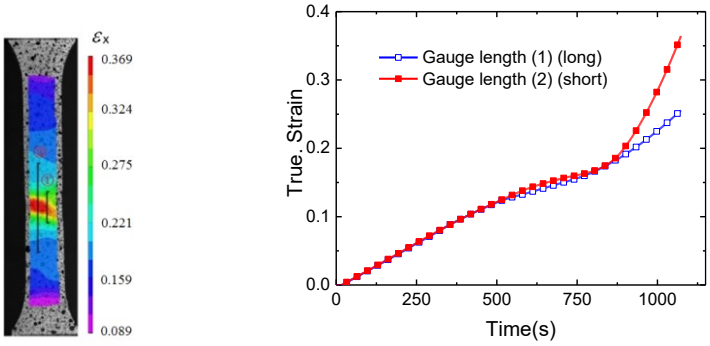

(a) (b)

Figure 4. Long and short gauge (a) used to average strain calculation (b).

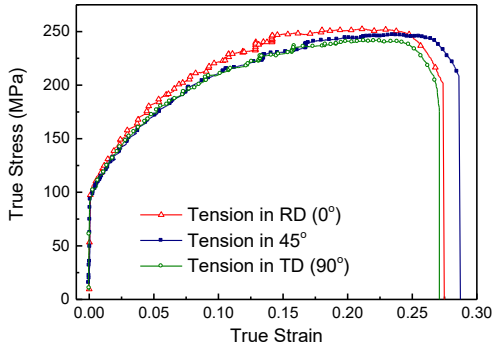

Figure 5. Stress-strain curves calculated from the recorded forces and DIC measured strains.

3.2. Results of ball punch deformation tests

By 3-D DIC program, the full-field strain distributions on the surface of ball punched sheets were measured. When the measured force declined larger than 5.0% during the test, the testing system perceived that the necking or fracture appeared on the deformed sheet and stopped the test. This method was proven to be reliable, for each tested sample was found exactly necked when the punching stopped. The dynamic strain fields obtained through DIC system are shown in Figure 6, and the limit strains were determined at the necking region through the inflection point of strain rate. Before the necking occurred, the strain concentrated at a ring belt near the dome apex, which was coincided with the description in Ref. [7].

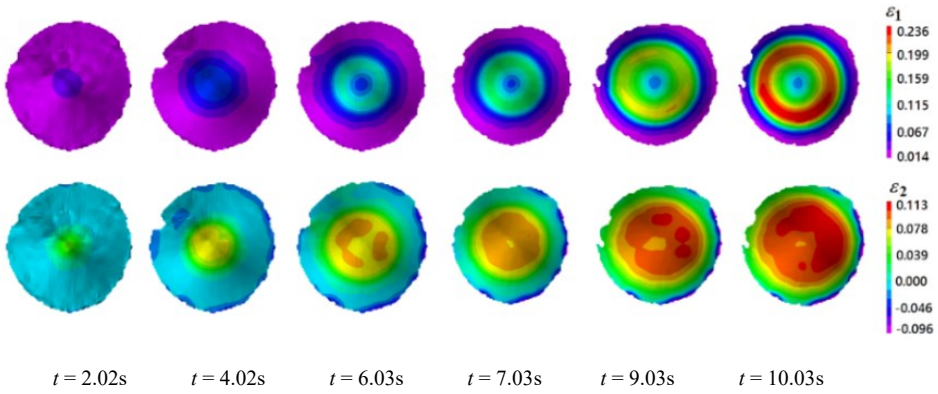

Figure 6. Major and minor strain filed measured by DIC, varying with the deformation time of sample 1# (equibiaxial stretching).

Figure 7 shows the final strain fields of six samples, where the necking all occurred. Owing to the distinctive shape and size, every test sample had different strain distributions (equal-biaxial, biaxial and uniaxial) on the outside surfaces.

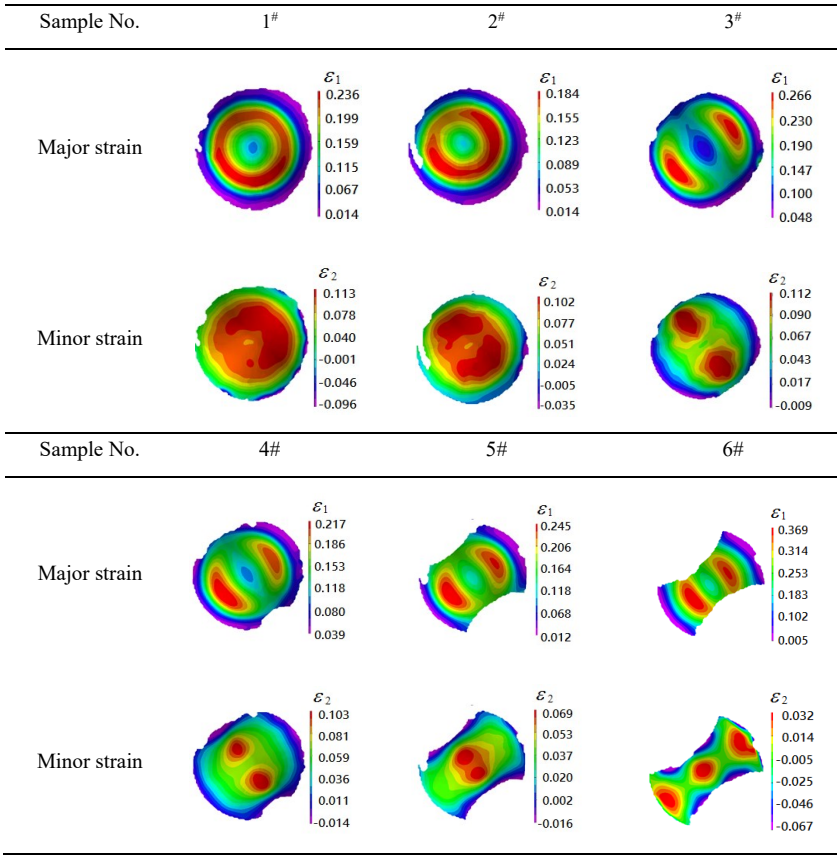

Figure 7. Major and minor strain filed when necking or fracture occurred in six samples.

Because the strain was real-time measured continuously, the limit strain can be determined easily. The CCD camera recorded the change of speckles during the forming. The comparison between the deformed speckles and the unformed speckles (references) can be used to calculate the distances and the strains of the speckles. Some featured points were selected on the surface of each test sample, which distributed at necking, safety and fracture areas, respectively. The strain states of these points were positioned in the minor strain-major strain coordinate system, and a forming limit curve (FLC) of aluminium alloy 5083 was constituted (Figure 8). This FLC of AA5083 was compared with that obtained by Bariani et al [9]. There is a good agreement in the FLC of AA5083 between the results of Bariani et al [9] and the present tests. FLD_0, the most critical points (the minor strain equals to zero in the plane strain state) in two tests were all near 0.16 and the slopes in the left and the right sides of FLC were also similar.

In the present tests, the punch was smaller than that recommended by the standard ISO12004-2 or ASTM E2218-02 (2008). A bending strain effect on the test metal sheet may occur, which contributes to a nonlinear strain path. When the limit strains were determined, strains at the necking region with various degrees were selected. Compared to the published FLC results of AA5083, most of the necking strains were larger. If the FLC was fitted with these necking strains, it will lift. In the present work, the lowest limit strain was selected to fit the FLC considering that the small punch was used.

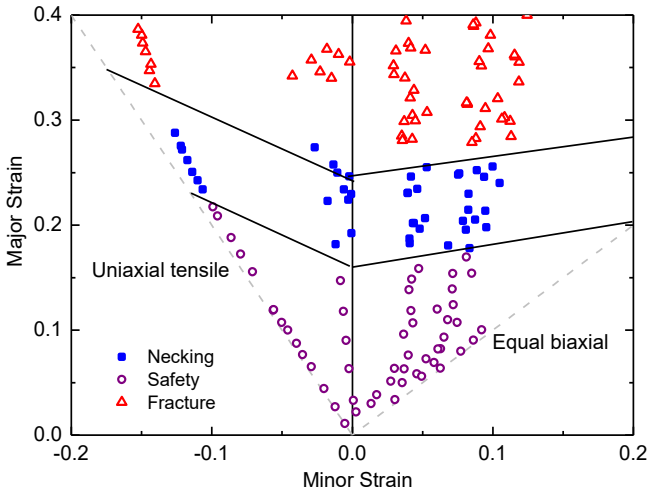

Figure 8. Forming limit diagram (FLD) generated from the measured strains by 3-D DIC.

3.3. Application of FLD

The deep drawing of the inner panel of a car body made of aluminium alloy 5083-O was finite element simulated. A commercial program AutoForm was used to build an FE model and perform the calculation. The material data including the FLD obtained from the experiments mentioned above were used. The objective of this simulation was validating the necking or fracture prediction of finite element simulation. The Hill's 48 yielding and flow rules were adopted, which was a simplified application for the complex constitutive equations needed more material constants. The friction coefficients between the metal sheet with the tooling was 0.015, which simulated the conditions of polyvinyl chloride (PVC) film applied in the forming experiments.

Figure 9 shows the simulation results, where the formability of materials was indicated by the color contour. The prediction results showed that two inner corners were prone to crack (red region) and inner side edge (yellow region) was thinned badly. The predicted defects was verified by the stamping experiment results as shown in Figure 10. Through the simulations using different parameters, it was found that poor lubrication was the main cause of forming defects. After improving the lubrication conditions, the inner panel was formed successfully.

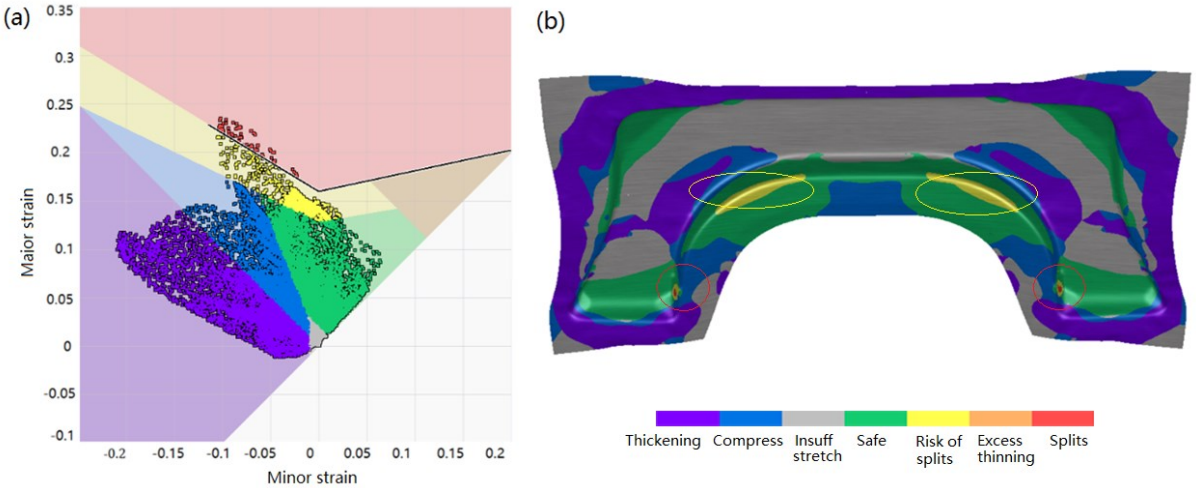

Figure 9. FE simulation results of the inner panel of an auto body. (a) FLD, (b) Simulated inner panel.

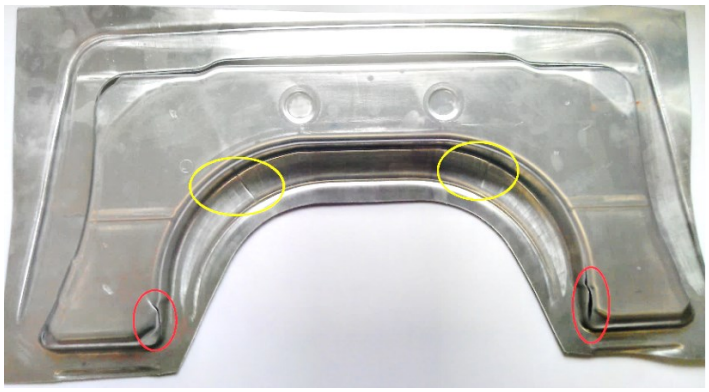

Figure 10. Experiment results of the inner panel of AA5083-O.

4. Conclusions

With the application of digital image correlation technology, the measurement accuracy of strain field of deformed aluminium alloy 5083-O sheet was improved. The dynamic strain field contributed to determining the strain to fracture in the uniaxial tensile tests, and the necking points on the dome regions of bulging tests were precisely located. The forming limit diagram of aluminium alloy 5083-O sheet was established. Based on these strain data and recorded load data, the damage and fracture of deformed sheet will be evaluated in the further research.

Acknowledgements

This research work was financially supported by the National Natural Science Foundation of China (No. 51375256).

References

[1] Sah S, Bawase M and Saraf M 2014 *SAE Technical Paper (***No. 2014-28-25)** 25-33.
[2] Hirsch J, 2014 *Trans. Nonferrous Met. Soc. China* **24** 1995−2002
[3] Khan A S and Baig M 2011 *Int. J. Plasticity* **27** 522-538.
[4] Abedrabbo N, Pourboghrat F and Carsley J 2006 *Int. J. Plasticity* **22** 342-373.
[5] Zhao J, Zeng P, Lei L and Ma Y 2012 *Opt. Laser Eng.* **50** 473-490.
[6] Wang K, Carsley J E, He B, Li J and Zhang L 2014 *J. Mater. Process. Tech.* **214** 1120-1130.
[7] Lu H and Cary P D 2000 *Exp. Mech.* **40** 393-400.
[8] Abedrabbo N, Pourboghrat F and Carsley J 2007 *Int. J. Plasticity* **23** 841-875.
[9] Bariani P F, Bruschi S, Ghiotti A and Michieletto F 2013 CIRP Ann-Mannuf. Tech. **62** 251-254.